

## Ultrathin low-frequency sound absorbing panels based on coplanar spiral tubes or coplanar Helmholtz resonators

Xiaobing Cai, Qiuquan Guo, Gengkai Hu, and Jun Yang

Citation: [Applied Physics Letters](#) **105**, 121901 (2014); doi: 10.1063/1.4895617

View online: <http://dx.doi.org/10.1063/1.4895617>

View Table of Contents: <http://scitation.aip.org/content/aip/journal/apl/105/12?ver=pdfcov>

Published by the [AIP Publishing](#)

---

### Articles you may be interested in

[The acoustic properties of panels with rectangular apertures](#)

J. Acoust. Soc. Am. **135**, 2777 (2014); 10.1121/1.4871363

[Discrete vortex model of a Helmholtz resonator subjected to high-intensity sound and grazing flow](#)

J. Acoust. Soc. Am. **132**, 2988 (2012); 10.1121/1.4757736

[Sound absorption and transmission through flexible micro-perforated panels backed by an air layer and a thin plate](#)

J. Acoust. Soc. Am. **131**, 3853 (2012); 10.1121/1.3701987

[A theoretical model to predict the low-frequency sound absorption of a Helmholtz resonator array](#)

J. Acoust. Soc. Am. **119**, 1933 (2006); 10.1121/1.2177568

[Helmholtz resonator with extended neck](#)

J. Acoust. Soc. Am. **113**, 1975 (2003); 10.1121/1.1558379

---



Automate your set-up with  
Miniature Linear Actuators

Affordable. Built-in controllers.  
Easy to set up. Simple to use.

**ZABER**

[www.zaber.com](http://www.zaber.com)



# Ultrathin low-frequency sound absorbing panels based on coplanar spiral tubes or coplanar Helmholtz resonators

Xiaobing Cai,<sup>1,2</sup> Qiuquan Guo,<sup>1</sup> Gengkai Hu,<sup>2</sup> and Jun Yang<sup>1,a)</sup>

<sup>1</sup>Department of Mechanical and Materials Engineering, The University of Western Ontario, London, Ontario N6A 5B9, Canada

<sup>2</sup>School of Aerospace Engineering, Beijing Institute of Technology, Beijing 100081, People's Republic of China

(Received 7 August 2014; accepted 1 September 2014; published online 22 September 2014)

Performance of classic sound absorbing materials strictly depends on their thickness, with a minimum of one-quarter wavelength to reach full sound absorption. In this paper, we report ultrathin sound absorbing panels that completely absorb sound energy with a thickness around one percent of wavelength. The strategy is to bend and coil up quarter-wavelength sound damping tubes into 2D coplanar ones, and embed them into a matrix to form sound absorbing panel. Samples have been designed and fabricated by 3D printing. Efficacies of sound absorption by these panels were validated through good agreement between theoretical analysis and experimental measurements.

© 2014 AIP Publishing LLC. [<http://dx.doi.org/10.1063/1.4895617>]

For decades, low-frequency sound absorption for noise mitigation remains challenging because the slow fluctuation of low-frequency acoustic waves leads to weak interaction between sound absorbing materials (SAMs) or structures and the viscous air medium, resulting in inefficient dissipation of sound energy.<sup>1,2</sup> Magnifying sound absorption at low-frequency usually needs either increasing wave path or field concentration.<sup>3–6</sup> To achieve a full absorption, a wave path no less than one quarter of wavelength is needed for classic SAMs,<sup>7–19</sup> while field intensifying is needed for resonant absorbers such as Helmholtz chambers, with required thicknesses still around one fourth of wavelength.<sup>20–22</sup> Recent advancements in metamaterials have inspired many unprecedented methods for materials designing and wave absorption, such as absorbing membrane,<sup>23,24</sup> omnidirectional absorber,<sup>25,26</sup> and coherent absorption.<sup>27,28</sup> In this paper, we present an ultrathin sound absorbing panel, comprising coplanar and coiled tubes or coplanar chambers, effectively absorbs low-frequency sound with a thickness less than one percent of wavelength.

The sketch of the panel comprising coplanar resonant tubes is illustrated in Fig. 1. From top view, these tubes are coiled up for space-saving purpose, with their axes twisted into spiral lines. The axes can also be any other curves, such as zigzag path, an effective method for obtaining high acoustic constitutive parameters based on “space-coiling” concept.<sup>29–31</sup> For simplicity, sectional shape of the tubes is square, while other types of sectional shapes are also acceptable. Starting from the adapting pores on the front covering board, the tubes are laid out in 2D space to allow sound waves smoothly propagating in.

The design of these coplanar tubes starts from analyzing sound absorption by an array of hollow tubes embedded in a rigid panel. Acoustic impedance at the opening of a tube with rigid termination can be expressed by  $Z_t = -iZ_c \cot(kL_t)$ , with  $L_t$ , the length of the tube;  $Z_c = (\rho/C)^{1/2}$ , the characteristic

impedance;<sup>2</sup> and  $k^2 = -\omega^2\rho C$ , the effective propagation constant. The effective density  $\rho$  and compressibility  $C$  are constitutional wave variables of this tube, and can be well calculated from visco-thermal acoustic theories.<sup>32–35</sup> For a panel containing an array of such tubes, the input impedance of sound wave for this panel can be estimated as  $Z_{in} = Z_t/\zeta$ , with  $\zeta = N\pi r_t^2/A$  being the porosity of the panel, where  $N$  is the number of tubes inside the panel within area  $A$ . Therefore, absorption of the panel can be determined by  $\alpha = 1 - |R|^2$ , where  $R$  is the reflectance and is determined by  $R = (Z_{in} - Z_{c0})/(Z_{in} + Z_{c0})$ ,<sup>2</sup> and  $Z_{c0}$  is the character impedance of air. Through the study, the term  $\cot(kL_t)$  signifies the quarter wavelength, which is a criterion for a tube to reach full absorption. The non-dimensional input impedance of the panel containing an array of tubes can be derived as  $Z_{in}/Z_{c0} = (Z_c/Z_{c0})[-i\cot(kL_t)/\zeta]$ . Full absorption requires impedance match between input impedance of the panel and the characteristic impedance of the air, i.e.,  $Z_{in}/Z_{c0} = 1$ . When radius of the tube  $r_t$  is big, such as on scale of millimetre, the first term  $(Z_c/Z_{c0})$  is close to 1.0. The term of  $\cot(kL_t)$  must approach to zero for case of small porosity  $\zeta$ , such as  $\zeta < 0.05$  in the case of present study. This yields to  $kL_t = \pi/2$ , i.e.,  $L_t \approx \lambda/4$ , where  $\lambda$  is the wavelength.

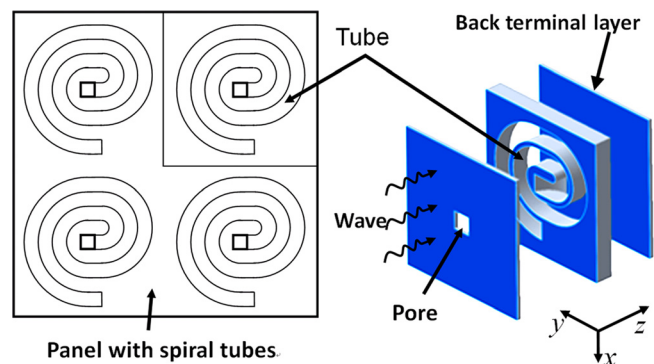


FIG. 1. The sketch of sound absorptive panel with arrays of embedded coplanar spiral tubes.

<sup>a)</sup>Author to whom correspondence should be addressed. Electronic address: [jiang@eng.uwo.ca](mailto:jiang@eng.uwo.ca). Tel.: 1-519-661-2111 ext. 80158. Fax: 1-519-661-3020

Figure 2 shows the relationship between the porosity and the radius when full absorption is achieved at a given frequency (e.g., 400 Hz) and when the tube length is one quarter of the corresponding wavelength ( $L_t = 205$  mm). As it reveals, SAMs comprising comparatively small pores require high porosity to reach unity absorption. Typical examples of such SAMs are glass wool, porous metal, etc., in which high porosity is necessary to generate more air flow frictions. On contrast, another category of SAMs require only low porosity to achieve full absorption when pore sizes are relatively large. This category of SAMs comprising structures like Helmholtz resonant chambers, generating full damping by acoustic resonance, where acoustic field is greatly intensified to promote sound energy dissipation. Nevertheless, both categories need thickness of the SAMs to be nearly one quarter wavelength to reach full absorption, no matter what the tube size is.

The strategy of this work, particularly applicable to the second category of SAMs, is to bend and wind the long, straight quarter-wavelength tubes into 2D coplanar tubes, and embed them in a thin panel. Therefore, the thickness of the sound absorbing panel can be greatly reduced, while its wave dissipation performance keeps the same.

The optimal thickness of the panel can be determined by considering its relation to tube size ( $r_t$ ) and porosity. To meet the dimension of a standard measurement system for sound absorption coefficient,<sup>36</sup> the panel samples were prepared in disk shape, with outer radius of  $R_0 = 30$  mm. The porosity of panel bearing these tubes thus can be calculated as  $\zeta = r_t^2/R_0^2$ , while thickness be around  $t \approx 2r_t$  (plus cover layer and back layer). The dashed curve in Fig. 2 reveals the dependence of porosity on tube size for leading to full absorption at a given frequency of 400 Hz. Combining with the relation of porosity and tube radius, i.e.,  $\zeta = r_t^2/R_0^2$ , it is easily to find the optimal tube size:  $r_t = 4.85$  mm. Accordingly, the optimal thickness of the panel is found to be  $t = 9.7$  mm. Substituting the relation of  $r_t = 0.5t$  into effective density  $\rho$  and compressibility  $C$  and further into  $Z_t$

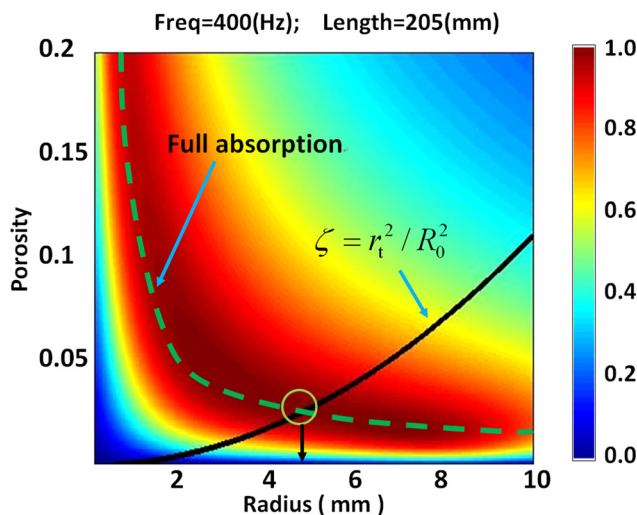


FIG. 2. The absorbing coefficient of 400 Hz sound waves by panel with tubes of 205 mm length for different panel porosities and tube sizes. The curves indicating full absorption and porosity/radius relation have been outlined.

and  $Z_{in}$ , dependence of sound absorption on panel thickness and tube length can be calculated and is shown in Fig. 3. The pair of tube length  $L_t = 205$  mm and panel thickness  $t = 9.7$  mm is found to be a unique solution for achieving full absorption at 400 Hz. Because the panel thickness is strictly related to tube radius and  $Z_t$  is inversely proportional to  $r_t^2$ ,<sup>10</sup> increasing or decreasing the panel thickness signifies enlarging or reducing the tube size, accordingly lowering down or raising up the impedance  $Z_t$ . This further makes the panel either less dissipative or less penetrable, as  $Z_{in} = Z_t/\zeta$ , where  $\zeta = r_t^2/R_0^2$ . In brief, as the impedance  $Z_{in}$  of the panel is inversely proportional to panel thickness, so only one solution allows impedance match, i.e.,  $Z_{in}/Z_{c0} = 1$ , a condition that is essential for achieving full absorption.

Figure 4(a) shows the fabricated samples by 3D printing. The tube sits inside a circular disk and is covered by a front layer (containing an adapting pore, see from Fig. 1) and a back terminal layer (not shown here, see from Fig. 1). The route of the tube's axis is spiral, yet can also be designed in other configurations. To facilitate the fabrication, here the cross section of the tube is square, with its side determined by  $a^2 = \pi r_t^2$ . The coplanar disk was mounted into impedance tube system to measure its sound absorbing coefficient by using standard transfer-function method.<sup>36</sup> Figure 5 shows the absorption coefficient curves of the disk in frequency range of 200 and 600 Hz. As predicted, full absorption occurs at around 400 Hz. Total thickness of the disk, including the front layer (3.4 mm) and back layers (5 mm), is about 17 mm; thus, the ratio of thickness to wavelength is about 1/50. Due to small fabrication error and surface roughness during 3D printing, the measured maximum absorption coefficient is about 0.9, slightly lower than 1.0. To further confirm that the energy dissipation is actually induced by and within the spiral tube, transmission loss of the sample is also measured. As shown by the dotted line in Fig. 5, the transmission of the sample is generally as low as 0.1, representing one percent of sound energy penetrate through the sample. As a comparison, transmission of a 5-mm-thick flat circular board is also measured and shown by the dashed line. As can be found, the transmission of the sample is close to but slightly lower than the flat board. The low

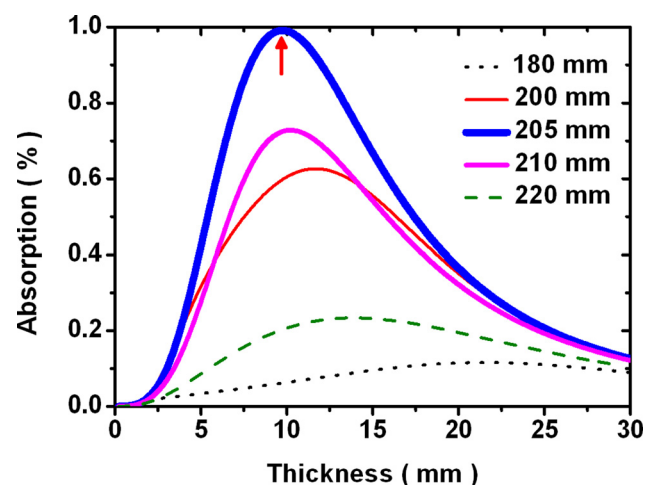


FIG. 3. The absorbing coefficients of 400 Hz sound waves by panel with spiral tubes for different thickness and tube length.

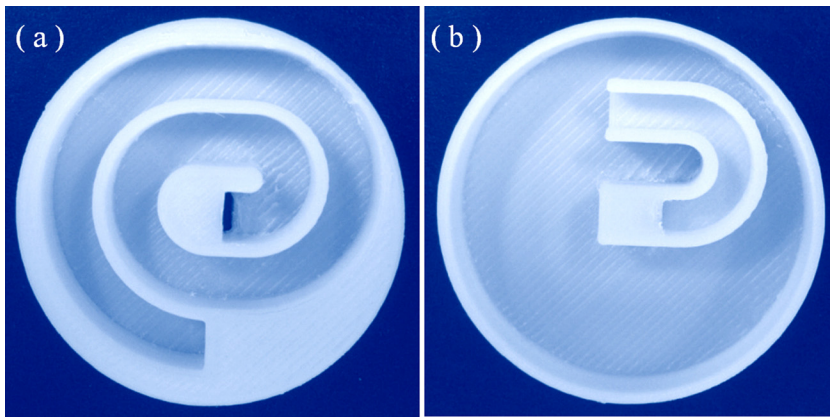


FIG. 4. Circular samples of sound absorbing panels with embedded (a) coplanar spiral tube and (b) coplanar resonant chamber fabricated by 3D printing technology (the diameter of the samples is 60 mm).

transmission is indeed generated by sound insulation of the back terminal layer. The contribution of transmission lost to absorption coefficient would be very small. Using energy conservation, the absorption coefficient can be modified as  $\alpha = 1 - |R|^2 - |T|^2$ , with  $T$  being the transmission coefficient. Only a tiny difference of 0.01 ( $|T|^2 \leq 0.01$ ) is needed to add into the absorption line in Fig. 5. Thus, we can conclude that the absorption peak at 400 Hz is solely caused by energy dissipation inside the sample, not by transmittance loss.

The velocity of the air flow driven by sound wave fluctuation has been found significantly increased near the tube opening when resonance occurs. As shown in Fig. 6, air flow speed reaches as high as 0.5 m/s at the resonant frequency of 400 Hz. While for sound wave slightly deviating from the resonant frequency, say 420 Hz, the maximum speed will sharply reduce to 0.05 m/s. Frictional force caused by the viscosity of the swift moving air would be at least 10 times larger at resonant state, thus greatly facilitates the dissipation of sound energy.

In resonant state, the movement of airflow in long coplanar tubes resembles that in a Helmholtz resonant chamber, so the coplanar tubes can be further evolved into planar Helmholtz resonant chambers. Figure 6 shows that the opening of the tube dominates the damping. In the rest part of the tube, no remarkable friction loss is generated, as air flow moves comparably slow there. Therefore, the inner section of the tube simply functions as the tank of a Helmholtz resonator,<sup>20</sup> while the opening section serves as the neck.

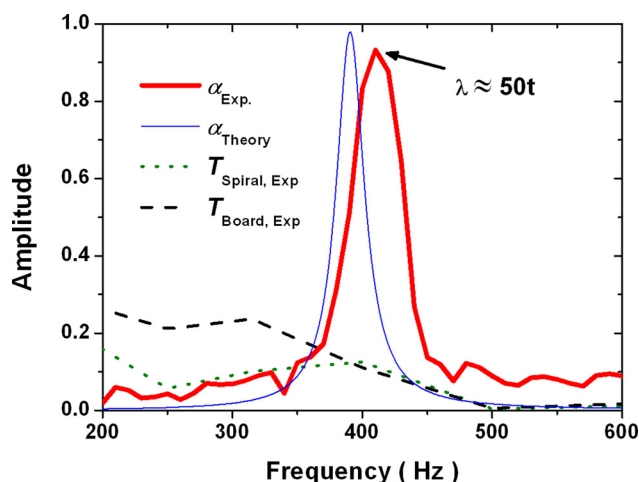


FIG. 5. The absorption and transmission coefficients of circular panel with embedded coplanar tube (Fig. 4(a)).

The planar Helmholtz resonator thus can be readily designed by keeping the opening section of the tube unchanged, while enlarging the inner section as much as possible. As an illustration, a disk sample containing the coplanar Helmholtz resonator is shown in Fig. 4(b). The resonator has a long narrow guiding tube ( $L = 50$  mm,  $a = 5.3$  mm) as the Helmholtz resonator's neck, while the rest space of the disk is removed to form its tank. The total thickness of the disk is 13.3 mm, with the front covering layer of 3 mm, back terminal layer 5 mm, and side wall of the tank of thickness 2 mm.

The predicted and measured sound absorption coefficients over frequency range of 100 Hz to 400 Hz are shown by the lines in Fig. 7. After changing the case of the long tubes (Fig. 4(a)) to the case of long neck Helmholtz resonators (Fig. 4(b)), the absorbing peak of the disk has shifted from previously 400 Hz to 250 Hz, without losing the capacity of unity absorption (although the measured absorption peak is slightly less than 1.0). The estimated ratio of disk thickness to wavelength is about 1/102. Compared with the above 1/50 for spiral tubes, this further thickness reduction benefits from the tank of the Helmholtz resonator taking better use of the space inside the disk, while the long neck still well fulfilling the task of consuming the sound energy by fierce flow friction. The Helmholtz resonator can also be seen as a “mass-spring” system. Since the volume of the tank is larger than that of the spiral tube (Fig. 4(a)), it

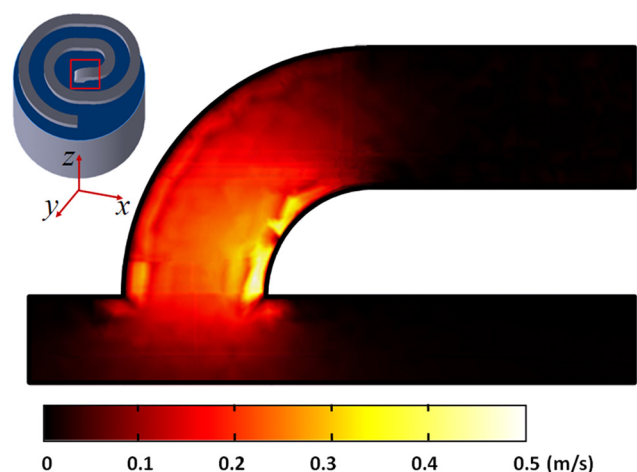


FIG. 6. The simulated air flow velocity distribution at resonant state near the opening of spiral tubes under fluctuation of sound wave.

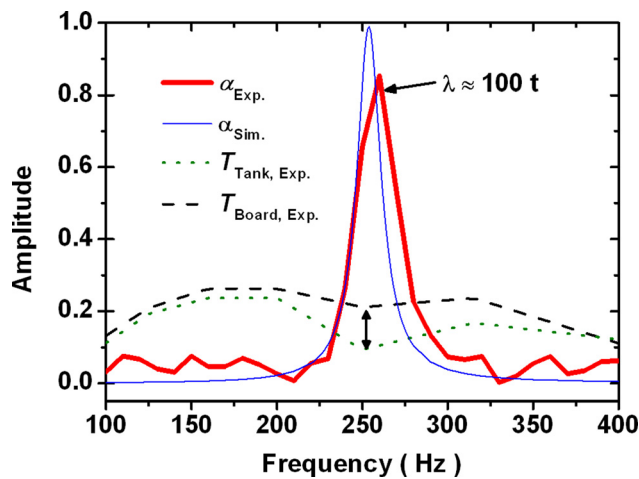


FIG. 7. The absorption and transmission coefficients of circular panel with embedded coplanar Helmholtz resonator (Fig. 4(b)).

represents a softer “spring” installed at the back of the “mass” (i.e., the neck). Accordingly, the resonant frequency of the “mass-spring” system lowers down. Transmission of the coplanar resonator is also measured and shown by the dotted line, which again is slightly lower than a 5-mm-thick flat board, as indicated by the dashed line. By comparing with that of the flat board, the transmission of the coplanar resonator drops from 0.2 to 0.15 near 250 Hz, which is an evidence of the energy absorption in the coplanar resonator. Considering the transmission of 0.2, its contribution to absorption coefficient would be less than 0.04. Again, we can confirm that the absorption peak of the panel is induced by sound energy dissipation, not by the transmittance loss.

A type of sound absorbing panel containing coplanar long tubes or coplanar Helmholtz resonant chambers has been designed, and demonstrated to have a resonant nature to fully absorb incident sound energy at low frequency. The thickness of the panel could be as small as one percent of the target sound wavelength. The mechanism of sound dissipation in this coplanar tube was investigated. With 3D printing technology for prototyping, and impedance tube for measuring sound absorbing coefficients, the sound absorption of designed panel was measured and the results agreed with the prediction. With this strategy, more practical sound absorbing panels can be designed for noise control applications.

This work was supported by Natural Science and Engineering Research Council of Canada (NSERC) and Research Accelerator Grant of The University of Western Ontario.

- <sup>1</sup>J. H. Conrad, *Engineering Acoustics and Noise Control* (Prentice Hall Inc., NJ, 1983).
- <sup>2</sup>J. F. Allard and N. Atalla, *Propagation of Sound in Porous Media: Modelling Sound Absorbing Materials* (Wiley, Chichester, 2009).
- <sup>3</sup>C. Wassilief, *Appl. Acoust.* **48**(4), 339–356 (1996).
- <sup>4</sup>T. J. Cox and P. D’Antonio, *Acoustic Absorbers and Diffusers: Theory, Design and Application* (Spon Press, London, 2004).
- <sup>5</sup>T. J. Lu, A. Hess, and M. F. Ashby, *J. Appl. Phys.* **85**(11), 7528–7539 (1999).
- <sup>6</sup>J. A. Moore and R. H. Lyon, *J. Acoust. Soc. Am.* **72**(6), 1989–1999 (1982).
- <sup>7</sup>M. P. Norton and D. G. Karczub, *Fundamentals of Noise and Vibration Analysis for Engineers, 2nd Ed.* (Cambridge University Press, Cambridge, 2003).
- <sup>8</sup>V. L. Jordan, *J. Acoust. Soc. Am.* **19**(6), 972–981 (1947).
- <sup>9</sup>S. Kim, Y. H. Kim, and J. H. Jang, *J. Acoust. Soc. Am.* **119**(4), 1933 (2006).
- <sup>10</sup>D. Y. Maa, *J. Acoust. Soc. Am.* **104**(5), 2861 (1998).
- <sup>11</sup>F. Hanl, G. Seiffert, Y. Zhao, and B. Gibbs, *J. Phys. D: Appl. Phys.* **36**(3), 294–302 (2003).
- <sup>12</sup>M. A. Biot, *J. Acoust. Soc. Am.* **28**(2), 168–178 (1956).
- <sup>13</sup>X. Wang and T. J. Lu, *J. Acoust. Soc. Am.* **106**(2), 756–765 (1999).
- <sup>14</sup>C. Perrot, F. Chevillotte, and R. Panneton, *J. Acoust. Soc. Am.* **124**(2), 940–948 (2008).
- <sup>15</sup>J. Liu and D. W. Herrin, *Appl. Acoust.* **71**(2), 120–127 (2010).
- <sup>16</sup>C. Wang and L. Huang, *J. Acoust. Soc. Am.* **130**(1), 208 (2011).
- <sup>17</sup>A. Scarpato, S. Ducruix, and T. Schuller, *J. Sound Vib.* **332**(20), 4856–4875 (2013).
- <sup>18</sup>S. H. Park, *J. Sound Vib.* **332**(20), 4895–4911 (2013).
- <sup>19</sup>K. Huang, D. Yang, S. He, and D. He, *J. Phys. D: Appl. Phys.* **44**(36), 365405 (2011).
- <sup>20</sup>U. Ingard, *J. Acoust. Soc. Am.* **25**(6), 1037–1061 (1953).
- <sup>21</sup>S. K. Tang, C. H. Ng, and E. Y. L. Lam, *Appl. Acoust.* **73**(9), 969–976 (2012).
- <sup>22</sup>A. Sanada and N. Tanaka, *Appl. Acoust.* **74**(4), 509–516 (2013).
- <sup>23</sup>J. Mei, G. Ma, M. Yang, Z. Yang, W. Wen, and P. Sheng, *Nat. Commun.* **3**, 756 (2012).
- <sup>24</sup>G. Ma, M. Yang, S. Xiao, Z. Yang, and P. Sheng, *Nat. Mater.* **13**, 873 (2014).
- <sup>25</sup>A. Climente, D. Torrent, and J. Sánchez-Dehesa, *Appl. Phys. Lett.* **100**, 144103 (2012).
- <sup>26</sup>R. Li, X. Zhu, B. Liang, Y. Li, X. Zou, and J. Cheng, *Appl. Phys. Lett.* **99**, 193507 (2011).
- <sup>27</sup>P. Wei, C. Croënne, S. T. Chu, and J. Li, *Appl. Phys. Lett.* **104**, 121902 (2014).
- <sup>28</sup>J. Song, P. Bai, Z. Hang, and Y. Lai, *New. J. Phys.* **16**, 033026 (2014).
- <sup>29</sup>Z. Liang and J. Li, *Phys. Rev. Lett.* **108**, 114301 (2012).
- <sup>30</sup>Z. Liang, T. Feng, S. Lok, F. Liu, K. B. Ng, C. H. Chan, J. Wang, S. Han, S. Lee, and J. Li, *Sci. Rep.* **3**, 1614 (2013).
- <sup>31</sup>Y. Xie, B. Popa, L. Zigoneanu, and S. A. Cummer, *Phys. Rev. Lett.* **110**, 175501 (2013).
- <sup>32</sup>H. Tijdeman, *J. Sound Vib.* **39**(1), 1–33 (1975).
- <sup>33</sup>M. R. Stinson, *J. Acoust. Soc. Am.* **89**(2), 550–558 (1991).
- <sup>34</sup>S. Scheichl, *J. Acoust. Soc. Am.* **115**(2), 534–555 (2004).
- <sup>35</sup>H. E. de Bree, F. J. M. van der Eerden, and J. W. van Honschoten, in *International Conference on Noise and Vibration, ISMA 25*, Leuven, 2000.
- <sup>36</sup>ISO 10534-2: 1998 Acoustics—Determination of Sound Absorption Coefficient and Impedance in Impedance Tubes—Part 2: Transfer-Function Method First Edition.